Journal of Physics: Conference Series **2586** (2023) 012001 doi:10.1088/1742-6596/2586/1/012001

Selected lattice QCD results on hadron structure

Constantia Alexandrou

Department of Physics, University of Cyprus, PO Box 20537, 1678 Nicosia, Cyprus, and
Computation-based Science and Technology Research Center, The Cyprus Institute, 20, Constantinou Kavafi Str., Nicosia 2121, Cyprus

E-mail: alexand@ucy.ac.cy

Abstract. We present recent results on hadron structure using lattice QCD simulations with physical values of the light, strange and charm quark masses. We overview progress on quantities that probe the three-dimensional structure of the nucleon focusing on recent results on Mellin moments and the direct computation of the x-dependence of parton distribution functions employing mainly the quasi-parton distribution approach within the large momentum effective theory.

1. Introduction

The theory of the strong interactions, Quantum Chromodynamics (QCD) proposed in 1973 [1], describes the amazingly rich structure of strongly interacting matter in the universe. In particular, it describes the emergence of hadrons, their structure and interactions. The proton, being a stable particle, has served for many years as a laboratory for studying the complex dynamics of QCD, both theoretically and experimentally. A key question that has been posed for many years is how the the properties of the proton, such as its spin, arise from its constituents, the quarks and the gluons, collectively called partons. Experimental efforts to understand the structure of the proton have been on-going for many decades and for example that proton electromagnetic form factors that are precisely determined in a range of momentum transfers. However, many others, such as the nucleon axial form factors, the distribution of quarks and gluons within the proton probing its three-dimensional (3D) structure, are still not well known. A rich experimental program is on-going in major facilities, such as JLab and CERN, to determine the 3D nucleon stucture that also constitutes the core of the science objectives of the Electron Ion Collider (EIC) being constructed at Brookhaven National Laboratory [2]. Such quantities include generalized parton distributions (GPDs) and transverse momentum dependent distributions (TMDs).

While experiments play a crucial role in probing the constituents of the nucleon, theoretical approaches to understand the 3D structure of hadrons are equally important. However, due to the non-perturbative nature of QCD, computing GPDs and TMDs is difficult. Lattice QCD provides the *ab initio* non-perturbative framework that is suitable to compute GPDs and TMDs using directly the QCD Lagrangian. Tremendous progress has been made in simulating lattice QCD in recent years. State-of-the-art simulations are currently being performed with dynamical up, down and strange quarks with masses tuned to their physical values. A subset of simulations also include a dynamical charm quark with mass fixed to approximately its physical value. A particularly suitable discretization scheme for studying hadron structure is the so called twisted mass fermion (TMF) action employed by the Extended Twisted Mass Collaboration (ETMC). The recent progress in simulating QCD was made possible using efficient algorithms and in particular multigrid solvers [3, 4] that were extended to twisted mass fermions [5]. In Fig. 1, we show the landscape of currently available gauge ensembles worldwide. As can be seen, ETMC and a number of other collaborations have ensembles generated with physical values of the pion mass, referred to as physical point ensembles. We also note that currently all ensembles are generated with lattice spacing $a > 0.05$ fm due to the so-called critical slow down of simulations. New approaches that include machine learning are being explored for addressing this issue.

The work-flow of a typical lattice QCD computation for baryon structure is shown schematically in Fig. 2. After defining the theory on a discrete finite 4-dimensional Euclidean lattice, one generates representative configurations of gauge links $U_\mu(x)$ via a Markov Chain Monte Carlo. The three-point correlation functions can be classified as connected when a probe couples to a valence quark and as disconnected when it couples to a sea quark or a gluon as shown in Fig. 2. Disconnected quark loop contributions require special techniques and larger computational resources. The generation of $U_\mu(x)$ together with the inversion of the Dirac matrix $D[U]$ to produce the quark propagator, are the most time consuming parts of the calculation. While the action $S[U]$ is local, det(D[U]) is not and it took years of algorithmic developments to be able to efficiently include it in the simulations. There are

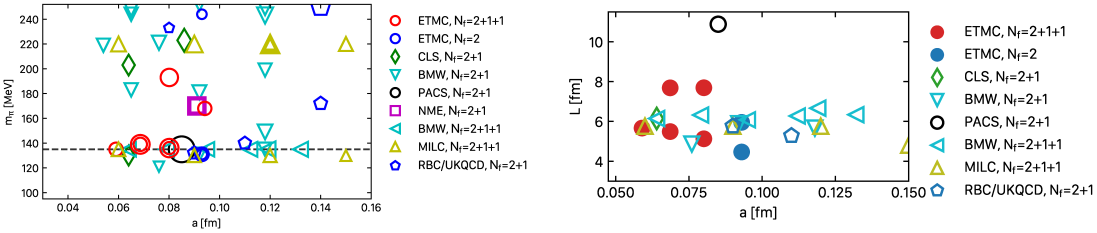

Figure 1. Left: Zero-temperature Gauge ensembles generated for studying hadron structure with a mass degenerate doublet of up and down quarks, referred to as light quarks and denoted as $N_f = 2$ ensembles, as well as with a strange quark ($N_f = 2 + 1$), and a charm quark ($N_f = 2 + 1 + 1$), as the mass of the light quarks is varied and as function of the lattice spacing a. The mass of the strange and charm quarks are tuned to approximately their physical values. The size of the symbol is proportional to the spatial extent of the lattice. Right: A summary of zero-temperature physical point ensembles by various lattice QCD collaborations as indicated by the legend for different spatial lengths L of the lattice as a function of a.

several discretization schemes for $D[U]$, each having its pros and cons. The most widely used are clover (employed e.g. by BMW, CLS, and PACS) and twisted mass fermions (ETMC), domain wall fermions (RBC/UKQCD) and staggered fermions (MILC) giving rise to the different collaborations mentioned in Fig. 1. All schemes coincide in the continuum limit.

Although lattice QCD provides an exact formalism for solving QCD, one needs a careful study of systematic errors. In the past, the absence of simulations at physical values of the light quark mass necessitated a chiral extrapolation. For the pion sector such an extrapolation using e.g. NLO SU(2) chiral perturbation theory works well for pion masses $m_\pi \lesssim 250$ MeV [6]. In the nucleon sector, chiral extrapolation is more problematic and introduces an uncontrolled systematic error [7]. Nowadays, with simulations with physical pion mass this systematic error can be eliminated. Therefore, in what follows we will focus on results obtained using simulation generated with physical pion mass, since we will focus on nucleon properties. Other systematic effects that need to be investigated include discretization and volume effects. An additional complication is the analysis of higher excited states that necessitates taking the large Euclidean time limit. Due to the increase of the gauge noise an identification of ground state properties can be difficult and requires large statistics. The development of noise reduction techniques is, thus, an important ongoing effort. The masses of the low-lying hadrons computed by the BMW collaboration using $N_f = 2 + 1$ ensembles and extrapolated to the continuum limit accounting as well as for finite volume effects yielded results in perfect agreement with the experimental values [8]. This ground breaking work was followed by the first computation from first principles also by BMW of the mass splitting of the proton and neutron and the identification of the isospin breaking contributions due to the difference in the masses of the u and d quarks and electromagnetism [9]. Beyond computing hadron masses, lattice QCD can be applied to study hadron matrix elements. Matrix elements computed in lattice QCD must be properly renormalized in order to compare with what is measured in the laboratory. In state-of-the-art lattice QCD computations, renormalization is carried out nonperturbatively. In what follows, we will present recent results on the two lowest Mellin moments of the nucleon that yield important information on e.g. the spin carried by quarks and gluons as well as new approaches to compute GPDs directly.

2. Mellin moments

GPDs are light-cone matrix elements that cannot be computed using a Euclidean formulation of QCD on which lattice simulations are based. Expansion of light-cone operators leads to a tower of local twist-2 operators that are connected to moments. The nucleon matrix elements of these local operators can be readily computed in lattice QCD. For zero momentum transfer squared they yield the following three

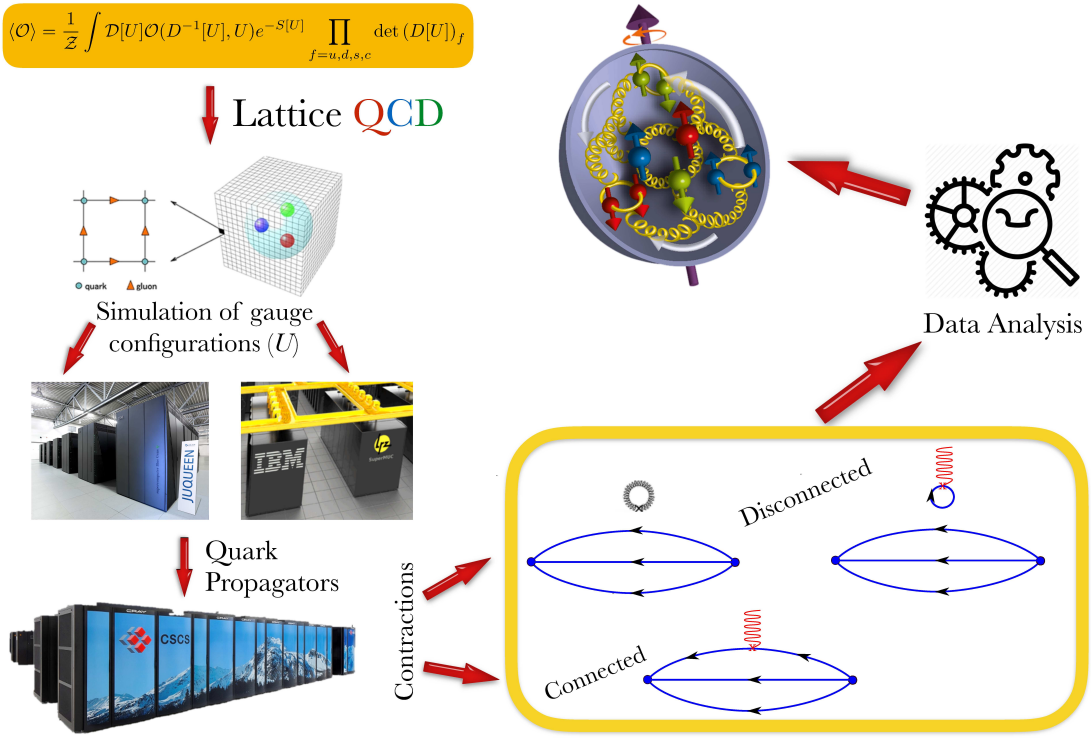

Figure 2. A typical work-flow for a baryon structure computation within lattice QCD. $S[U]$ is the action in Euclidean time and the integration is over the gauge links U. The expectation value of an appropriately defined operator O yields the physical properties we are interested in. The diagrams shown in the lower right box correspond to the connected and disconnected three-point correlators needed for baryon structure studies.

moments of PDFs:

$$O^{\mu_1\ldots\mu_n} = \bar{\psi}\gamma^{\{\mu_1} iD^{\mu_2}\ldots iD^{\mu_n\}}\psi \quad \overset{unpolarized}{\rightarrow} \quad \langle x^n\rangle_q = \int_0^1 dx\, x^n \left[q(x) - (-1)^n \bar{q}(x)\right]\rangle$$

$$\tilde{O}^{\mu_1\ldots\mu_n} = \bar{\psi}\gamma_5\gamma^{\{\mu_1} iD^{\mu_2}\ldots iD^{\mu_n\}}\psi \quad \overset{helicity}{\rightarrow} \quad \langle x^n\rangle_{\Delta q} = \int_0^1 dx\, x^n \left[\Delta q(x) + (-1)^n \Delta\bar{q}(x)\right]$$

$$O_T^{\rho\mu_1\ldots\mu_n} = \bar{\psi}\sigma^{\rho\{\mu_1} iD^{\mu_2}\ldots iD^{\mu_n\}}\psi \quad \overset{transversity}{\rightarrow} \quad \langle x^n\rangle_{\delta q} = \int_0^1 dx\, x^n \left[\delta q(x) - (-1)^n \delta\bar{q}(x)\right],$$

where $q = q_\downarrow + q_\uparrow$, $\Delta q = q_\downarrow - q_\uparrow$, $\delta q = q_\intercal + q_\perp$. For non-zero momentum transfer we obtain moments of GPDs that can be expanded in term of generalized form factors (GFFs). As an example, we give the moments of the unpolarized GPDs E and H:

$$\int_{-1}^1 dx\, x^{n-1} H(x,\xi,\tau) = \sum_{i=0,2,\cdots}^{n-1} \left[(2\xi)^i A_{ni}(\tau) + \mathrm{mod}(n,2)(2\xi)^n C_{n0}(\tau)\right]$$

$$\int_{-1}^1 dx\, x^{n-1} E(x,\xi,\tau) = \sum_{i=0,2,\cdots}^{n-1} \left[(2\xi)^i B_{ni}(\tau) - \mathrm{mod}(n,2)(2\xi)^n C_{n0}(\tau)\right],$$

where x is the momentum fraction, $\tau = -Q^2 = (p'-p)^2$ is the momentum transfer squared and $\xi = \frac{p^+ - p'^+}{2P^+}$ the skewness. Here we will only consider the two lowest moments $n = 1, 2$. For $n = 1$ we obtain the

nucleon form factors, which at $Q^2 = 0$ give the vector, axial and tensor charges. The isovector vector charge $g_V^{u-d} = 1$ by symmetry. The axial charge g_A is well measured from β-decay and a number of lattice QCD collaborations have computed it. The value quoted by FLAG [10] that averages over lattice QCD results agrees with the experimental value. On the other hand, the isovector tensor charge g_T^{u-d} is less well measured. In Fig. 3 we show recent lattice results compared to those extracted from phenomenology. As can be seen, lattice QCD yields an accurate value that be use as input in phenomenological analysis of transversity as done recently by the JAM collaboration [11]. Allowing momentum transfer yields for $n = 1$ the form factors. In Fig. 3, we show the strange nucleon electromagnetic form factors, demonstrating that sea quark effects can be accurately determined and showing non-zero strangeness in the nucleon.

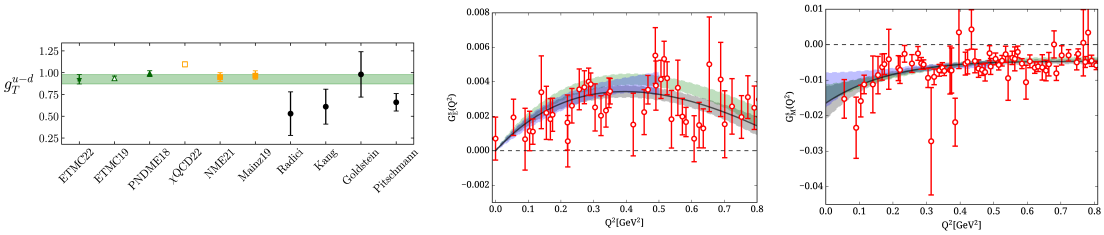

Figure 3. Lattice results on g_T^{u-d} (left) from: ETMC [12, 13] using only physical mass point ensembles, PNDME [14], χQCD [15], NME [16], and CLS-Mainz [17] (green symbols for $N_f = 2 + 1 + 1$ and yellow for $N_f = 2 + 1$ ensembles). Open green and yellow symbols denote lattice QCD results without continuum extrapolation. Results from phenomenology are shown with the black circles [18, 19, 20, 21]. The strange electric (middle) and magnetic (right) nucleon form factors (red circles) computed using one ensemble by ETMC [22].

In order to study the spin carried by quarks in the nucleon, we need the second moment of the unpolarized GPD given by

$$\langle N(p',s')|O^{\mu\nu,q}|N(p,s)\rangle = \bar{u}_N(p',s')\Big[A_{20}^q(q^2)\gamma^{\{\mu}P^{\nu\}} + B_{20}^q(q^2)\frac{i\sigma^{\{\mu\alpha}q_\alpha P^{\nu\}}}{2m} + C_{20}^q(q^2)\frac{q^{\{\mu}q^{\nu\}}}{m}\Big]u_N(p,s)$$

For $Q^2 = 0$, we obtain the quark spin $J_q = \frac{1}{2}\left[A_{20}^q(0) + B_{20}^q(0)\right]$ and momentum fraction $\langle x\rangle_q = A_{20}^q(0)$, with equivalent expressions for the gluon. In Fig. 4, we show our results for the proton average momentum fraction for the up, down, strange and charm quarks, for the gluons, as well as their sum [23, 24]. The up quark makes the largest quark contribution of about 35% and it is twice as big as that of the down quark. The strange quark contributes significantly less, namely about 5% and the charm contributes about 2%. Fig. 4, showing connected and disconnected contributions, demonstrates that disconnected contributions are crucial and if excluded would result to a significant underestimation of the momentum sum.

All quark flavors together constitute to about 60% of the proton spin. The gluon contribution is as significant as that of the up quark, namely about 45% providing the "missing" spin. Summing all the contributions results to

$$\sum_{q=u,d,s,c}\langle x\rangle_q + \langle x\rangle_g = 1.045(118) \text{ and } \sum_{q=u,d,s,c} J_q + J_g = 0.47(7),$$

confirming indeed the momentum and spin sums. The $\sum_{q=u,d,s} B_{20}^{q^+}(0) + B_{20}^g(0)$ is expected to vanish in order to respect the momentum and spin sums. We find for the renormalized values that $\sum_{q=u,d,s} B_{20,R}^{q^+}(0) + B_{20,R}^g(0) = -0.099(91)(28)$, which is indeed compatible with zero.

Since the quark contribution to the proton total angular momentum is computed, it is interesting to examine how much comes from the intrinsic quark spin. In Fig. 5 we show our results for the intrinsic

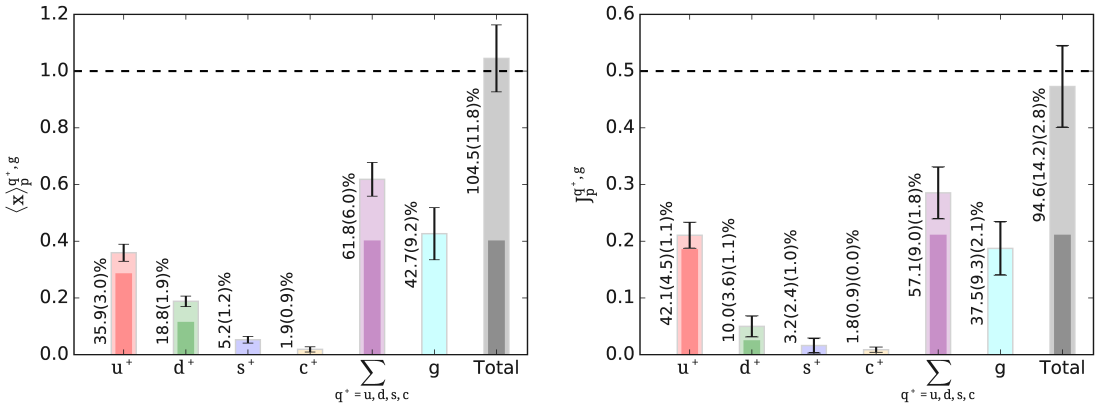

Figure 4. The decomposition of the proton average momentum fraction $\langle x \rangle_P$ (left) and spin J_P [23, 24]. We show the contribution of the up (red bar), down (green bar), strange (blue bar) and charm (orange bar) quarks and their sum (purple bar), the gluon (cyan bar) and the total sum (grey bar). Note that what is shown is the contribution of both the quarks and antiquarks ($q^+ = q + \bar{q}$). Whenever two overlapping bars appear the darker bar denotes the purely connected contribution while the light one is the total contribution, which includes disconnected taking into account also the mixing. The error bars on the only connected part are omitted while for the total are shown explicitly on the bars. The percentages written in the figure are for the total contribution. The dashed horizontal line is the momentum and spin sums. Results are given in $\overline{\text{MS}}$ scheme at 2 GeV.

quark spin $\frac{1}{2}\Delta\Sigma^{q^+} = \frac{1}{2}g_A^{q^+}$, where g_A^q is the axial charge for each quark, the values of which are taken from Ref. [12]. The up quark has a large contribution of about 85% of the proton intrinsic spin. The down quark contributes about half compared to the up and with opposite sign. The strange and charm quarks also contribute negatively with the latter being about five times smaller than the former giving a 1% contribution. The total $\frac{1}{2}\Delta\Sigma^{q^+}$ is in agreement with the upper bound from COMPASS [25].

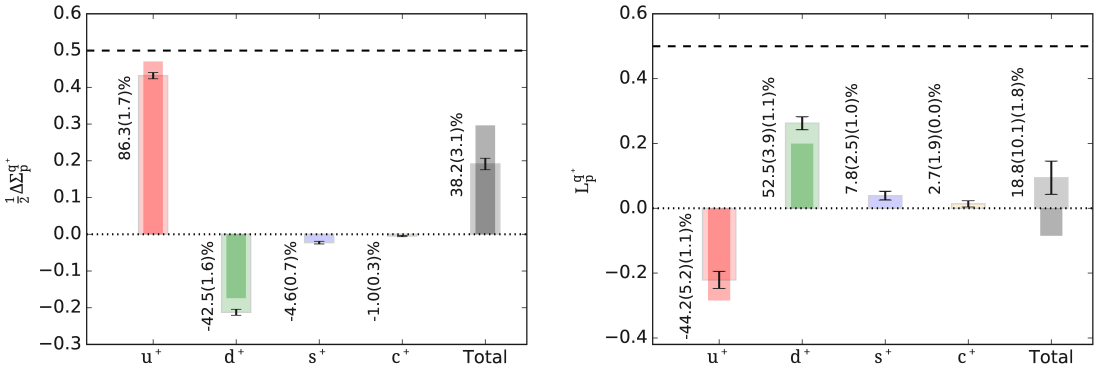

Figure 5. Results for the intrinsic quark spin $\frac{1}{2}\Delta\Sigma$ (left) and orbital angular momentum L (right) in the $\overline{\text{MS}}$ scheme at 2 GeV [12, 23, 24]. The notation is the same as that of Fig. 4.

Having both the quark total angular momentum and the quark intrinsic spin allows us to extract the orbital angular momentum L_q. Our results are shown in Fig. 5. The orbital angular momentum of the up quark is negative reducing the total angular momentum contribution of the up quark to the proton spin. The contribution of the down quark to the orbital angular momentum is positive almost canceling the negative intrinsic spin contribution resulting to a relatively small positive contribution to the spin of the proton. For a direct calculation of L_P using TMDs see Ref. [26].

3. Direct computation of x-dependence of parton distributions

While for many years only GFFs were accessible in lattice QCD, a new approach was proposed that enables us to compute the x-dependence of parton distribution functions (PDFs) and GPDs within lattice QCD taking advantage of the so-called large momentum effective theory (LaMET) [27]. The main idea is to compute spatial correlators in lattice QCD, e.g. along the z-axis and boost the nucleon state in the same direction to large momentum. After renormalization, a matching kernel computed perturbatively is used to recover the light-cone correlation matrix element. In this presentation, we will present results using mostly the quasi-PDF approach for which there have been many studies. For recent reviews see Refs. [28, 29, 30, 31]. The starting point is the renormalized space-like matrix elements for boosted nucleon states

$$\tilde{F}_\Gamma(x, P_3, \mu) = 2P_3 \int_{-\infty}^{\infty} \frac{dz}{4\pi} e^{-ixP_3 z} \langle P_3 | \overline{\psi}(0)\, \Gamma W(0,z)\, \psi(z) | P_3 \rangle |_\mu \quad ,$$

where W is a Wilson line and $\Gamma = \gamma_0, \gamma_i\gamma_5$ and $\sigma_{i,j}, i \neq j$, for the unpolarized, helicity and transversity PDFs, respectively. The quasi-PDF $\tilde{F}_\Gamma$ is then matched using a perturbatively compute kernel to extract the light-cone PDF $F_\Gamma(x, \mu)$. For details we refer to Refs. [32, 33].

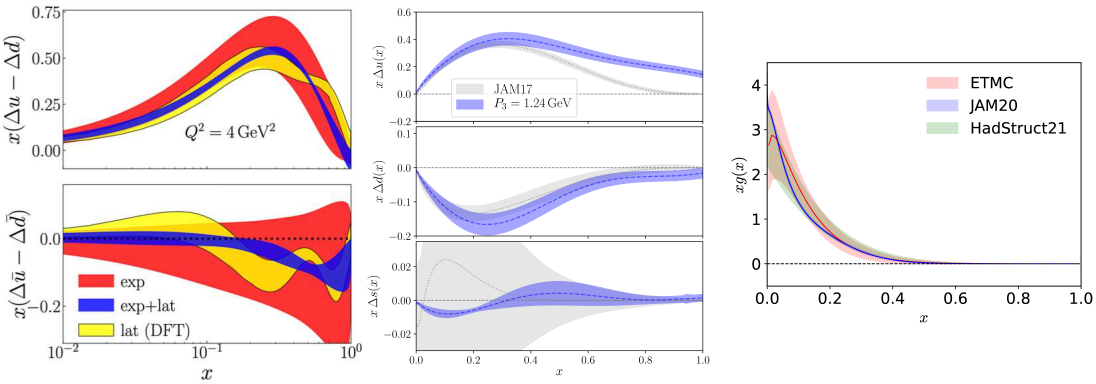

Figure 6. Left: Isovector helicity PDF. We show lattice results by ETMC (yellow) and results from a phenomenological analysis by the JAM17 [34] without (red) and with (blue) lattice input on g_T^{u-d}. Middle: The up (top), down (middle) and strange (bottom) quark helicity PDF (blue) versus x in the $\overline{\mathrm{MS}}$ scheme at 2 GeV computed using an $N_f = 2 + 1 + 1$ TMF ensemble by ETMC with pion mass $m_\pi = 260$ MeV (blue) [35]. We compare with results from a phenomenological analysis by JAM17 (grey) [34]. Right: The unpolarized PDF determined by the HadStruc collaboration [36] (green band) and ETMC (red band) using the pseudo-PDF approach compared to phenomenology by JAM20 (blue) [37].

Results using an $N_f = 2+1+1$ twisted mass fermion physical point ensemble for the isovector helicity PDF are shown in Fig. 6 together with comparison to phenomenological results. As can be seen, using the lattice determination of g_T^{u-d} increases the accuracy in the extraction of phenomenological results. To determine the flavor decomposition of PDFs one needs to compute, besides the isovector, the isoscalar PDFs. The latter as well as the strange PDFs involve disconnected contributions. These are computed by extending the formalism developed for local operators to extended operators. The up, down and strange helicty PDFs are shown in Fig. 6 [35, 38], computed for an ensemble of $N_f = 2 + 1 + 1$ TMF simulated with pion mass of 260 MeV. This computation demonstrates that they can be determine with good accurancy within lattice QCD. The computation using physical point ensembles is ongoing. The unpolarized gluon PDF can be extracted by computing the matrix elements of a spin-averaged nucleon for two gluon fields connected by a Wilson line, using Wilson flow to redues ultraviolet fluctuations. A first determiantion of the unpolarized gluon PDF is done by the HadStruc Collaboration followed by ETMC using gauge ensembles simulated with about 350 MeV pion and results are shown in Fig. 7. The pseudo-PDF approach, a variation of the quasi-PDF method, is used that avoids the computation of the renormalization factor.

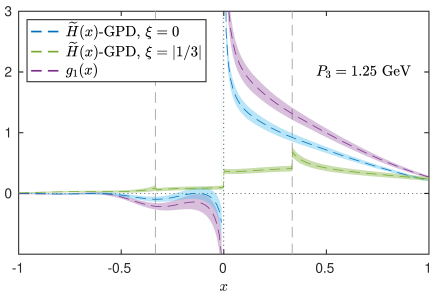

Figure 7. The helicity GPD computed by ETMC [39].

The quasi-PDF approach can be extended to study GDPs, where momentum transfer is involved. One computes the nucleon matrix element

$$h_\Gamma(z, \tilde{\xi}, Q^2, P_3) = \langle N(P_3\hat{e}_z + \vec{Q}/2)|\,\overline{\psi}(z)\,\Gamma W(z,0)\,\psi(0)|\,N(P_3\hat{e}_z - \vec{Q}/2)\rangle,$$

where the quasi-skewness $\tilde{\xi} = -\frac{Q_3}{2P_3} = \xi + O(\frac{1}{P_3^2})$ with ξ the skewness [39]. Results on the helicity GPD are shown in Fig. 7 computed for an ensemble of $N_f = 2 + 1 + 1$ TMF simualted with pion mass of 260 MeV, for $\xi = 0$ and $\xi = 1/3$.

4. Conclusions

Moments of PDFs as well as form factors can be extracted precisely making these quantities part of the precision era of lattice QCD. From these moments we can extract a lot of interesting physics and also reconstruct the PDFs, as it was demonstrated for the pion [40]. Sea quark effects can be accurately studied within lattice QCD as illustrated by the computation of the strange electromagnetic form factors. New theoretical approaches (quasi-distributions, pseudo-distributions, current-current correlators, etc) are being employed for the direct computation of PDFs within lattice QCD yielding very promising results including calculations using gauge ensembles generated with physical pion mass. The calculation of sea quark contributions to PDFs is shown to be feasible providing valuable input e.g. for the determination of the strange helicity PDF. Exploratory studies of isovector GDPs are also under way, see e.g. recent studies by ETMC [39, 41, 42]. The way forward includes studying the continuum limit and the volume dependence and developing noise reduction techniques to reach larger boosts. Extending these approaches to twist-3 PDFs [43], TMDs, and other hadrons is also in the pipeline.

Acknowledgments

I am thankful to the members of ETMC for their important contributions in many of the topics presented. Special thanks to S. Bacchio, M. Constantinou, J. Finkenrath, K. Hadjiyiannakou, K. Jansen and G. Koutsou. We acknowledge support by the Cyprus Research and Innovation Foundation under contract numbers POST-DOC/0718/0100 and COMPLEMENTARY/0916/0015, the project "Nucleon parton distribution functions using Lattice Quantum Chromodynamics" funded by the University of Cyprus, and the European Joint Doctorate projects HPC-LEAP and STIMULATE funded by the European Union's Horizon 2020 research and innovation programme under grant agreement No 642069 and 765048, respectively. We also acknowledge the Gauss Centre for Supercomputing (GCS) e.V. (www.gauss-centre.eu) by providing computing time on SuperMUC at Leibniz Supercomputing Centre (www.lrz.de) under project pr74yo, Piz Daint at Centro Svizzero di Calcolo Scientifico (CSCS), via the project with id s702 and the Extreme Science and Engineering Discovery Environment (XSEDE), which is supported by National Science Foundation grant number TG-PHY170022. We acknowledge Temple University for providing computational resources, supported in part by the National Science Foundation (Grant Nr. 1625061) and by the US Army Research Laboratory (contract Nr. W911NF-16-2-0189). This work used computational resources from the John von Neumann-Institute for Computing on the Jureca system at the research center in Jülich, under the project with id ECY00.

References

[1] H. Fritzsch, M. Gell-Mann and H. Leutwyler, Phys. Lett. B **47** (1973), 365-368.
[2] A. Accardi, *et al.* Eur. Phys. J. A **52** (2016) no.9, 268 [arXiv:1212.1701 [nucl-ex]].

[3] A. Frommer, K. Kahl, S. Krieg, B. Leder and M. Rottmann, SIAM J. Sci. Comput. **36** (2014), A1581-A1608 [arXiv:1303.1377 [hep-lat]].
[4] M. A. Clark, B. Joó, A. Strelchenko, M. Cheng, A. Gambhir and R. Brower, [arXiv:1612.07873 [hep-lat]].
[5] C. Alexandrou, S. Bacchio and J. Finkenrath, Comput. Phys. Commun. **236** (2019), 51-64 [arXiv:1805.09584 [hep-lat]].
[6] S. Dürr, PoS **LATTICE2014** (2015), 006 [arXiv:1412.6434 [hep-lat]].
[7] G. Colangelo, A. Fuhrer and S. Lanz, Phys. Rev. D **82** (2010), 034506 [arXiv:1005.1485 [hep-lat]].
[8] S. Durr *et al.*, Science 322 (2008) 1224.
[9] Sz. Borsanyi *et al.*, Science 347 (2015) 1452.
[10] Y. Aoki *et al.* [Flavour Lattice Averaging Group (FLAG)], Eur. Phys. J. C **82** (2022) no.10, 869 [arXiv:2111.09849].
[11] L. Gamberg *et al.* [Jefferson Lab Angular Momentum (JAM) and Jefferson Lab Angular Momentum], Phys. Rev. D **106** (2022) no.3, 034014 [arXiv:2205.00999 [hep-ph]].
[12] C. Alexandrou, S. Bacchio, M. Constantinou, J. Finkenrath, K. Hadjiyiannakou, K. Jansen, G. Koutsou and A. Vaquero Aviles-Casco, Phys. Rev. D **102** (2020) no.5, 054517 [arXiv:1909.00485 [hep-lat]].
[13] C. Alexandrou, *et al.* [arXiv:2202.09871 [hep-lat]].
[14] R. Gupta, Y. C. Jang, B. Yoon, H. W. Lin, V. Cirigliano and T. Bhattacharya, Phys. Rev. D **98** (2018), 034503 [arXiv:1806.09006 [hep-lat]].
[15] D. Horkel *et al.* [χQCD], Phys. Rev. D **101** (2020) no.9, 094501 [arXiv:2002.06699 [hep-lat]].
[16] S. Park *et al.* [Nucleon Matrix Elements (NME)], Phys. Rev. D **105** (2022) no.5, 054505 [arXiv:2103.05599 [hep-lat]].
[17] T. Harris, G. von Hippel, P. Junnarkar, H. B. Meyer, K. Ottnad, J. Wilhelm, H. Wittig and L. Wrang, Phys. Rev. D **100** (2019) no.3, 034513 [arXiv:1905.01291 [hep-lat]].
[18] M. Radici and A. Bacchetta, Phys. Rev. Lett. **120** (2018) no.19, 192001 [arXiv:1802.05212 [hep-ph]].
[19] Z. B. Kang, A. Prokudin, P. Sun and F. Yuan, Phys. Rev. D **93** (2016) no.1, 014009 [arXiv:1505.05589 [hep-ph]].
[20] G. R. Goldstein, J. O. Gonzalez Hernandez and S. Liuti, [arXiv:1401.0438 [hep-ph]].
[21] M. Pitschmann, C. Y. Seng, C. D. Roberts and S. M. Schmidt, Phys. Rev. D **91** (2015), 074004 [arXiv:1411.2052].
[22] C. Alexandrou, S. Bacchio, M. Constantinou, J. Finkenrath, K. Hadjiyiannakou, K. Jansen and G. Koutsou, Phys. Rev. D **101** (2020) no.3, 031501 [arXiv:1909.10744 [hep-lat]].
[23] C. Alexandrou, S. Bacchio, M. Constantinou, J. Finkenrath, K. Hadjiyiannakou, K. Jansen, G. Koutsou, H. Panagopoulos and G. Spanoudes, Phys. Rev. D **101** (2020) no.9, 094513 [arXiv:2003.08486 [hep-lat]].
[24] C. Alexandrou, M. Constantinou, K. Hadjiyiannakou, K. Jansen, C. Kallidonis, G. Koutsou, A. Vaquero Avilés-Casco and C. Wiese, Phys. Rev. Lett. **119** (2017) no.14, 142002 [arXiv:1706.02973 [hep-lat]].
[25] C. Adolph *et al.* [COMPASS], Phys. Lett. B **753** (2016), 18-28 [arXiv:1503.08935 [hep-ex]].
[26] M. Engelhardt, Phys. Rev. D **95** (2017) no.9, 094505 [arXiv:1701.01536 [hep-lat]].
[27] X. Ji, Phys. Rev. Lett. **110** (2013), 262002 [arXiv:1305.1539].
[28] H. W. Lin, *et al.* Prog. Part. Nucl. Phys. **100** (2018), 107-160 [arXiv:1711.07916 [hep-ph]].
[29] M. Constantinou, *et al.* Prog. Part. Nucl. Phys. **121** (2021), 103908 [arXiv:2006.08636 [hep-ph]].
[30] X. Ji, Y. S. Liu, Y. Liu, J. H. Zhang and Y. Zhao, Rev. Mod. Phys. **93** (2021) no.3, 035005.
[31] K. Cichy, [arXiv:2111.04552 [hep-lat]].
[32] C. Alexandrou, K. Cichy, M. Constantinou, K. Jansen, A. Scapellato and F. Steffens, Phys. Rev. Lett. **121** (2018) no.11, 112001 [arXiv:1803.02685 [hep-lat]].
[33] C. Alexandrou, K. Cichy, M. Constantinou, K. Jansen, A. Scapellato and F. Steffens, Phys. Rev. D **98** (2018) no.9, 091503 [arXiv:1807.00232 [hep-lat]].
[34] J. J. Ethier, N. Sato and W. Melnitchouk, Phys. Rev. Lett. **119** (2017) no.13, 132001 [arXiv:1705.05889 [hep-ph]].
[35] C. Alexandrou, M. Constantinou, K. Hadjiyiannakou, K. Jansen and F. Manigrasso, Phys. Rev. Lett. **126** (2021) no.10, 102003 [arXiv:2009.13061 [hep-lat]].
[36] T. Khan, *et al*. (HadStruc Collaboration) Phys. Rev. D 101 (2021) 094516, [arXiv:2107.08960 [hep-lat]].
[37] J. Cammarota *et al.* [Jefferson Lab Angular Momentum], Phys. Rev. D **102** (2020) no.5, 054002 [arXiv:2002.08384].
[38] C. Alexandrou, S. Bacchio, M. Constantinou, K. Hadjiyiannakou, K. Jansen and G. Koutsou, Phys. Rev. D **104** (2021), 074503 [arXiv:2106.13468 [hep-lat]].
[39] C. Alexandrou, K. Cichy, M. Constantinou, K. Hadjiyiannakou, K. Jansen, A. Scapellato and F. Steffens, Phys. Rev. Lett. **125** (2020) no.26, 262001 [arXiv:2008.10573].
[40] C. Alexandrou *et al.* [ETM], Phys. Rev. D **104** (2021) no.5, 054504 [arXiv:2104.02247 [hep-lat]].
[41] C. Alexandrou, K. Cichy, M. Constantinou, K. Hadjiyiannakou, K. Jansen, A. Scapellato and F. Steffens, Phys. Rev. D **105** (2022) no.3, 034501 [arXiv:2108.10789 [hep-lat]].
[42] A. Scapellato, C. Alexandrou, K. Cichy, M. Constantinou, K. Hadjiyiannakou, K. Jansen and F. Steffens, PoS **LATTICE2021** (2022), 129 [arXiv:2111.03226 [hep-lat]].
[43] S. Bhattacharya, K. Cichy, M. Constantinou, A. Metz, A. Scapellato and F. Steffens, Phys. Rev. D **102** (2020) no.11, 111501 [arXiv:2004.04130 [hep-lat]].